0013-7227/02/$15.00/0
Printed in U.S.A.

The Journal of Clinical Endocrinology & Metabolism 87(1):226–234

Fatty Acid-Induced Insulin Resistance: Decreased Muscle PI3K Activation But Unchanged Akt Phosphorylation

YOLANTA T. KRUSZYNSKA, DOROTHY SEARS WORRALL, JACHELLE OFRECIO, JUAN P. FRIAS, GINA MACARAEG, AND JERROLD M. OLEFSKY

Department of Endocrinology and Metabolism, University of California San Diego, Veterans Administration Center, La Jolla, California 92093

The mechanisms by which elevated plasma nonesterified fatty acid (NEFA) levels induce skeletal muscle insulin resistance remain unclear. A NEFA-induced defect in the activation of PI3K, which plays a key role in insulin's stimulation of glucose transport, has been invoked. We sought to examine the effects of elevated plasma NEFA (~1 mmol/liter) on muscle PI3K activity, insulin receptor substrate (IRS)-1 (important for activation of PI3K), and Akt, which is downstream of PI3K and activated by phosphorylation on serine and threonine in a PI3K-dependent manner. Ten normal men [age, 37 ± 9 yr (mean ± SD); body mass index, 25.2 ± 3.8 kg/m^2] underwent two 5-h hyperinsulinemic (80 mU/m^2·min) euglycemic clamps with basal and end of clamp biopsies of the vastus lateralis muscle. Plasma NEFAs were increased in one study by infusion of 20% Intralipid (1 ml/min) and heparin (900 U/h) throughout and for 2.5 h beforehand. Skeletal muscle protein levels were quantified by Western blotting. Elevated plasma NEFA reduced whole-body insulin-stimulated glucose disposal by 24% (42.1 ± 4.0 *vs.* 54.8 ± 3.6 μmol/kg·min; $P < 0.001$). Basal muscle IRS-1 was the same in the two studies. IRS-1 levels decreased by 40% in the control glucose clamps ($P < 0.005$), but did not change during the Intralipid study. Total tyrosine phosphorylated IRS-1 increased by 29% during the control clamps ($P < 0.05$), but by only 18% (NS) during the Intralipid studies. Total levels of p85α subunit of PI3K and Akt were not influenced by plasma NEFA levels either in the basal state or during the glucose clamps. The insulin-induced increase in IRS-1-associated PI3K activity was impaired by elevated NEFA, so that activity at the end of the clamps with Intralipid was 35% lower than in the control clamps ($P < 0.05$). The percentage reduction in PI3K activation correlated with the reduction in insulin-stimulated glucose disappearance rate that was induced by elevated NEFA ($r = 0.70$; $P < 0.05$). Basal P-ser- and P-thr-Akt levels were very low and unaffected by NEFA levels. The glucose clamps resulted in a marked increase in P-ser and P-thr Akt levels. Despite the decrease in PI3K in the Intralipid study, no defect in Akt phosphorylation was found. In summary, NEFA-induced insulin resistance is associated with an impairment of IRS-1 tyrosine phosphorylation and IRS-1-associated PI3K activation. Down-regulation of IRS-1 levels is also impaired. The NEFA-induced defect in muscle glucose uptake appears to be a consequence of a defect in the insulin-signaling pathway leading to impaired PI3K activation. This in turn may lead to impaired glucose transport through an Akt-independent pathway because Akt phosphorylation was unaffected by elevated NEFA levels. (*J Clin Endocrinol Metab* 87: 226–234, 2002)

ELEVATED PLASMA NONESTERIFIED fatty acid (NEFA) levels have been implicated in the pathogenesis of insulin resistance (1–3). Fasting plasma NEFA levels have been found to correlate inversely with insulin sensitivity in nondiabetic subjects (4, 5), and in nondiabetic Pima Indians they are predictive of the subsequent development of type 2 diabetes (6). Increased NEFA availability results in decreased rates of glucose oxidation (7–9) and inhibits insulin-stimulated skeletal muscle glycogen deposition (7) and whole-body glucose uptake by 15–50% (3, 7, 8, 10–14). However, although inhibition of glucose oxidation is seen with little delay, the defect of insulin-mediated glucose disposal is manifested after 3 h or more of raised NEFA levels (7, 8, 11, 15).

Competition between glucose and fatty acids for oxidative metabolism is largely explained by the inhibitory effects of elevated NEFA on pyruvate dehydrogenase and on glycolysis, as demonstrated by Randle *et al.* (16). They postulated that inhibition of muscle glycolysis would increase glucose-6-phosphate levels, which in turn would inhibit hexokinase and, hence, phosphorylation and uptake of glucose. However, it is now apparent that decreased glucose uptake must involve additional direct inhibitory effects of NEFA on insulin-stimulated glucose transport. Evidence for this came from the finding that when plasma NEFAs were elevated during a hyperinsulinemic glucose clamp in normal subjects, gastrocnemius muscle glucose-6-phosphate levels, instead of increasing, as would be expected if the defect in glucose uptake was secondary to a block in glycolysis, progressively decreased (7, 17); the decline preceded the defect in glycogen deposition (7, 17). Intracellular free glucose levels were lower when NEFAs were elevated (12), implying a primary defect in the pathway by which insulin stimulates glucose transporter 4 (Glut 4) translocation and glucose transport.

Binding of insulin to its receptor activates the intrinsic tyrosine kinase, which initiates a cascade of cell-signaling responses, including the phosphorylation of insulin receptor substrate (IRS) proteins that act as docking proteins (18). The most abundant and perhaps most important of these in terms

Abbreviations: Glut 4, Glucose transporter 4; HGO, hepatic glucose output; IR-β, insulin receptor β-subunit; IRS, insulin receptor substrate; N, nitrogen; NEFA, nonesterified fatty acid; PI, phosphatidylinositol; PI-3-P, PI-3-phosphate; Ra, rate of appearance; Rd, rate of disappearance.

of insulin signaling in human muscle is IRS-1. Tyrosine phosphorylation of IRS-1 permits its association with the regulatory subunit of PI3K. This in turn activates PI3K activity, which is necessary for insulin signaling to glucose transport (18, 19). The mechanism by which activated PI3K induces Glut 4 translocation and increased glucose uptake has not been defined. A downstream effector of PI3K is the serine-threonine kinase, PKB (Akt). It may play a role in insulin's effects on glucose transport (20, 21), although this is controversial (22).

Gumbiner *et al.* (13) found no effect of elevated NEFAs on insulin binding to muscle insulin receptors or on their kinase activity, suggesting that the NEFA-induced defect in insulin signaling to glucose transport is downstream of the insulin receptor. By contrast, in cultured mouse myoblasts, palmitate led to a 50% decrease in insulin-induced tyrosine phosphorylation of the insulin receptor β-subunit (IR-β) (23). Only two *in vivo* studies, one in rats and another in humans, have examined the effects of elevated NEFA on muscle insulin-signaling steps distal to the receptor (12, 24). Both studies found that NEFA-induced insulin resistance was associated with impaired activation of muscle PI3K by insulin (12, 24). In rats, this defect was associated with decreased tyrosine phosphorylation of IRS-1 (24). In the human study, levels of insulin-signaling proteins or their phosphorylation state were not examined (12).

Mean plasma NEFA levels in the lipid-infused rats studied by Griffin *et al.* (24) were rather high at 2.8 mmol/liter. At these levels, direct effects on cell membranes and integral membrane proteins might be anticipated. The aim of our study was therefore to examine the effects of a more physiological elevation of plasma NEFA (~1 mmol/liter), similar to that found in obesity and type 2 diabetes, on proximal insulin-signaling steps in muscle of healthy male subjects, and in particular, to examine the relationships between effects of elevated NEFA on basal and insulin-stimulated IRS-1, PI3K, and Akt. To do this, muscle biopsies were taken in the basal state and at the end of a 5-h hyperinsulinemic euglycemic clamp performed with and without elevated plasma NEFA levels.

Materials and Methods

Subjects

Ten healthy male subjects [age, 37.4 ± 8.7 (SD) yr; weight, 77.0 ± 14.1 kg; body mass index, 25.2 ± 3.8 kg/m^2] with normal glucose tolerance were studied. The study was approved by the Human Subjects Internal Review Board of the University of California, San Diego; written informed consent was obtained from each subject. None were on treatment known to affect glucose tolerance. All consumed a diet containing at least 200 g carbohydrate per day.

Protocol

Each subject was admitted to the University of California San Diego Clinical Research Center in the evening on three occasions approximately 5–10 d apart. Studies were performed in the morning after a 10- to 12-h overnight fast. Each subject underwent the following three studies in random order: 1) a control 5-h 80 mU/m^2·min hyperinsulinemic euglycemic clamp with biopsy of the vastus lateralis muscle before and at the end of the clamp; 2) a 5-h 80 mU/m^2·min hyperinsulinemic euglycemic clamp study with elevated plasma NEFA and muscle biopsy at the end of the clamp; 3) a muscle biopsy taken in the basal state after elevation of plasma NEFA. Plasma NEFAs were elevated in studies 2 and 3 for 7.5 h by infusion of a triglyceride emulsion containing 21 g/liter of glycerol as emulsifier (Intralipid 20%; Fresenius Kabi Clayton, Clayton, NC) and heparin. The fatty acid composition of Intralipid is 52% linoleate, 13% palmitate, 22% oleate, 4.5% stearate, and 8.5% other. The Intralipid (60 ml/h) and heparin (900 U/h) infusions were started 2.5 h before the glucose clamp and continued during the clamp in study 2; in study 3, they were started at 0100 h, 7.5 h before performance of the muscle biopsy. The heparin infusion was discontinued 30 min before the muscle biopsies, whereas the Intralipid infusion was continued until the end of the procedure.

Hyperinsulinemic euglycemic clamps

At 0400 h, an 18-gauge cannula was inserted in an antecubital vein, and a constant infusion of 3-^{3}H-glucose (0.25 μCi/min) (NEN Life Science Products, Boston, MA) was started. For blood sampling, a venous cannula was inserted retrograde into a distal forearm vein, the hand being maintained in a hand warmer at 70 C. After each blood sample was taken, this cannula was flushed with 0.15 mol/liter NaCl in water. After four basal blood samples were taken at 0800 h for estimation of plasma glucose concentration and specific activity, insulin, NEFA, and triglyceride levels, an iv infusion of insulin (Humulin S, Eli Lilly & Co., Indianapolis, IN) diluted in 0.15 mol/liter saline containing 1% wt/vol human albumin was begun at 80 mU/m^2·min from a Harvard syringe pump. Potassium and phosphate were given iv to compensate for the intracellular movement of these ions and to maintain normal serum levels. Blood glucose was measured at 5-min intervals, and the blood glucose concentration was clamped at 5.0 mmol/liter for 5 h by adjustment of the rate of infusion of a solution of 20% (wt/vol) glucose in water (25). Blood samples for glucose concentration and specific activity were taken every 20 min until +270 min, and then every 10 min until +300 min.

Muscle biopsies (200–300 mg) were obtained from the vastus lateralis under local lignocaine anesthesia (26). On the control study day, a biopsy was taken before the basal blood samples and again at 300 min of the glucose clamp. The clamp was prolonged beyond 300 min until completion of the muscle biopsy. Corresponding basal and end of clamp muscle biopsies during the clamp with elevated NEFA were taken on separate days as detailed above. Tissue was blotted free of blood and immediately frozen in liquid nitrogen (N), under which it was stored until used for studies of the IR-β, IRS-1, PI3K, and Akt.

Whole-body glucose and lipid oxidation

Substrate oxidation rates in the basal state and during the glucose clamps were determined by indirect calorimetry, using the Metascope II calorimeter (Cybermedic Inc., Boulder, CO). Briefly, a clear plastic ventilated hood was placed over the subject's head, and room air was drawn through the hood at a constant rate of 35–50 liter/min. Oxygen consumption and CO_2 production were measured for 15 min during the second half of each 30 min of the study, and the means of the values during the last 10 min of the measurement interval were used for calculations. A timed (approximately 5 h) basal urine sample was obtained, and a further sample was obtained at the conclusion of the study for determination of urinary N excretion rates during the basal and clamp periods. Nonprotein respiratory quotient was calculated from the rates of O_2 consumption, CO_2 production, and urinary N excretion as previously described (27). Carbohydrate and lipid oxidation were calculated from standard equations (27). In some subjects, negative rates of lipid oxidation were observed during the glucose clamp. These negative values are thought to be numerically equivalent to the net amount of lipid synthesized (28). Under conditions of lipogenesis, the standard equation (glucose oxidized = 4.55 VCO_2 − 3.21 VO_2 − 2.87 N, where VCO_2 is CO_2 production and VO_2 is O_2 consumption) overestimates the amount of glucose oxidized by an amount equal to that converted to fat (28). Therefore, when negative rates of lipid oxidation were obtained, glucose oxidation was calculated from the following equation (28):

$$\text{Glucose oxidized} = 1.34\,(1.00\ VCO_2 - 4.88\ \text{N})$$

Total nonoxidative glucose disposal during the glucose clamp was calculated by subtracting the amount of glucose oxidized and the glucose excreted in the urine from total plasma glucose disappearance rate (Rd).

Muscle IRS-1 immunoprecipitation and Western blotting of muscle proteins

Muscle samples (30–50 mg) were homogenized (Polytron Kinematica, Lucerne, Switzerland) in 1.5 ml ice-cold buffer [50 mmol/liter HEPES (pH 7.4), 150 mmol/liter sodium chloride, 200 mmol/liter sodium fluoride, 20 mmol/liter sodium pyrophosphate, 4 mmol/liter sodium vanadate, 10% vol/vol glycerol, 0.85% vol/vol Triton X-100, 2 mmol/liter phenylmethylsulfonylfluoride, and two Complete protease inhibitor tablets per 100 ml] (Roche Molecular Biochemicals, Mannheim, Germany). After 15 min on ice, the samples were centrifuged for 5 min at 2,500 rpm (1,000 × *g*). Then, the supernatants were centrifuged at 14,000 × *g* for 20 min (4 C). The protein concentration in the supernatant was determined using the Bio-Rad Laboratories, Inc. (Hercules, CA) protein assay kit, and the samples were diluted with the above buffer to a final protein concentration of 3 mg/ml. Then, aliquots were diluted with an equal volume of 2× Laemmli buffer containing 100 mmol/liter dithiothreitol, heated at 98 C for 6 min, and stored at −70 C until used for Western blotting. For immunoprecipitation of IRS-1, the muscle extracts (1.0 mg protein in 1.0 ml) were incubated at 4 C on a rotating mixer with 8 μg anti-IRS-1 antibody for 2 h and 2% vol/vol protein A Sepharose for a further 12 h. For subsequent Western blot analysis, the immunoprecipitates were washed three times with the above buffer, resuspended in Laemmli sample buffer with 100 mmol/liter dithiothreitol, and heated at 98 C for 6 min. Immunoprecipitated proteins and proteins in the total muscle extracts prepared above (45 μg protein per lane) were separated by SDS-PAGE (5 or 7.5% resolving gel) and transferred to Immobilon P membranes (Millipore Corp., Bedford, MA) in 39 mmol/liter glycine, 48 mmol/liter Tris, 0.0375% wt/vol SDS, 20% methanol using a semi-dry blotting apparatus (Pharmacia-LKB multiphor II system) at a constant current of 1.2 mA/cm^2 for 90 min. Preliminary experiments were conducted to determine for each of the proteins studied that the amount of homogenate protein loaded was within a range that resulted in a proportionate change in signal intensity as the amount of protein loaded was varied.

Aliquots (3–12 μg protein) of a standard 3T3-L1 lysate preparation were run in parallel on all gels. Membranes were blocked for 1 h at room temperature with 5% nonfat dry milk or with 2.5% BSA (for RC20 antibody blots) and then incubated at 4 C overnight with the following antibodies: rabbit anti-IR-β (Santa Cruz Biotechnology, Inc., Santa Cruz, CA), rabbit anti-IRS-1 or mouse monoclonal antibody against the p85α subunit of PI3K, (both from Upstate Biotechnology, Inc., Lake Placid, NY), rabbit antibodies to Akt (recognizes Akt-1, Akt-2, and Akt-3 isoforms), to ser 473 phosphorylated Akt and to thr-308 phosphorylated Akt (all from New England Biolabs, Inc., Beverly, MA). After washing, the membranes were incubated at room temperature with either antimouse or antirabbit horseradish peroxidase-conjugated secondary antibodies as appropriate. To quantify tyrosine phosphorylated IRS-1, membranes were incubated overnight at 4 C with a primary antibody that was conjugated with horseradish peroxidase (RC20, Transduction Laboratories, Lexington, KY). Then, membranes were washed again, and bands were visualized using enhanced chemiluminescence (Pierce Chemical Co., Rockford, IL) and quantified by densitometry.

PI3K assay

Skeletal muscle IRS-1 was immunoprecipitated with anti-IRS-1 antibody and protein A Sepharose beads as described above. The bead pellets were washed three times with buffer A [Tris-buffered saline (pH 7.4) containing 1% vol/vol Nonidet P-40, 100 μmol/liter Na_3VO_4], three times with buffer B [100 mmol/liter Tris HCl (pH 7.4) containing 500 mmol/liter $LiCl_2$, 100 μmol/liter Na_3VO_4], and twice with buffer C [10 mmol/liter Tris HCl (pH 7.4) containing 100 mmol/liter NaCl, 1 mmol/liter EDTA, 100 μmol/liter Na_3VO_4]. The beads were suspended in 10 mmol/liter Tris HCl (pH 7.4) containing 100 mmol/liter NaCl, 1 mmol/liter EDTA, 10 mmol/liter $MgCl_2$, 100 μmol/liter EGTA, and 20 μg phosphatidylinositol (PI). PI3K activity was measured in a final reaction volume of 100 μl by the phosphorylation of PI in the presence of 20 μCi [γ-^{32}P]ATP for 20 min (29). The reactions were terminated by the addition of 20 μl 8 M HCl, and then the lipids were extracted with 160 μl chloroform:methanol (1:1 vol/vol). The organic phase was loaded on to *trans*-1,2-diaminocyclohexane-N,N,N′,N′-tetra-acetic acid (1% wt/vol) -coated silica gel TLC plates. After the separation of lipids by TLC using the boric acid method (30), PI-3-phosphate (PI-3-P) was visualized by autoradiography. Signals were quantitated by densitometric scanning. PI3K activity is expressed in arbitrary units relative to the signal intensity of a standard muscle sample processed in parallel and loaded on each TLC plate.

Other analyses

Plasma glucose was measured by a glucose oxidase method immediately after sampling using a model 2700 Yellow Springs analyser (YSI, Inc., Yellow Springs, OH). For determination of ^{3}H glucose specific activity, 0.65 ml plasma was deproteinized with $Ba(OH)_2/ZnSO_4$ (31). After centrifugation, the neutral supernatant was evaporated, and the residue was dissolved in 1 ml water. After adding 10 ml of scintillation fluid (Ecoscint, Manville, NJ), ^{3}H dpm were determined in an ICN 36014 liquid scintillation counter (Titertek Instruments, Inc., Huntsville, AL) using an external standard to correct for quenching. Quadruplicate aliquots of the labeled glucose infusate were added to nonradioactive plasma and processed in parallel with the plasma samples to allow calculation of the 3-^{3}H-glucose infusion rate.

Serum insulin was measured by a double antibody technique (32). The intra- and interassay coefficients of variation were 6.8 and 7.9%, respectively. Urinary N excretion was calculated from the urine concentrations of creatinine, uric acid, and urea (33). Blood (1.0 ml) for determination of plasma NEFA was taken into EDTA-coated microfuge tubes and immediately centrifuged (10 sec, 14,000 × *g*) in an Eppendorf (Hamburg, Germany) microcentrifuge; the plasma was immediately frozen on solid CO_2. Plasma samples were stored at −70 C until assayed.

Calculation of glucose appearance and disappearance rates

In the basal state, rates of glucose appearance (Ra) and disappearance (Rd) were calculated by dividing the 3-^{3}H-glucose infusion rate by the plasma glucose specific activity using the mean of the four basal plasma samples. During the clamp, glucose Ra and Rd were calculated from the 3-^{3}H-glucose data using the non-steady state equations of Steele *et al.* (34). A distribution volume of 0.19 liter/kg and a pool fraction of 0.5 were used in the calculation (35). Hepatic glucose output (HGO) was calculated by subtracting the exogenous glucose infusion rate from glucose Ra.

Statistical analysis

Results are expressed as mean ± SEM unless otherwise indicated. The significance of differences within groups was tested by paired *t* test or, in the case of the Western blot data and PI3K activities, by the Wilcoxon paired sample test because these data were not normally distributed. Correlations were sought by Pearson's least squares method. A *P* value less than 0.05 was considered statistically significant.

Results

Plasma glucose, insulin, NEFA, and triglyceride concentrations

Fasting plasma glucose concentrations were not affected by infusion of Intralipid and heparin (Table 1). In the control study, fasting plasma NEFA levels were 0.34 ± 0.05 mmol/liter and were suppressed to very low levels during the glucose clamps (Table 1). Infusion of Intralipid and heparin raised fasting plasma NEFA levels approximately 3-fold, and these elevated levels were maintained throughout the glucose clamps (Table 1). Fasting triglyceride levels were increased approximately 2-fold by the Intralipid and heparin infusion (Table 1), and increased further to 362 ± 73 mg/dl by the last half hour of the glucose clamp. By contrast, in the control studies plasma triglyceride levels decreased to a mean level of 95 ± 21 mg/dl during the last half hour of the glucose clamps. Fasting insulin levels and insulin levels dur-

TABLE 1. Plasma glucose, insulin, and lipid levels in the basal state and during the last 30 min of the 80 mU/m^2·min hyperinsulinemic euglycemic clamps performed in the absence (control) and presence of an infusion of Intralipid and heparin (lipid) in 10 normal male subjects

	Control		Lipid	
	Basal	Clamp	Basal	Clamp
Plasma glucose (mmol/liter)	5.0 ± 0.1	5.0 ± 0.0	5.0 ± 0.1	5.1 ± 0.0
Plasma insulin (pmol/liter)	54 ± 12	696 ± 42	66 ± 12	714 ± 36
Plasma NEFA (μmol/liter)	340 ± 46	14 ± 4	1042 ± 62[a]	966 ± 129[a]
Serum triglyceride (mg/dl)	126 ± 22	95 ± 21	283 ± 47[b]	362 ± 73[a]

Values are expressed as mean ± SEM.
[a] $P < 0.001$, [b] $P < 0.002$, compared to levels in the same state on the control study day.

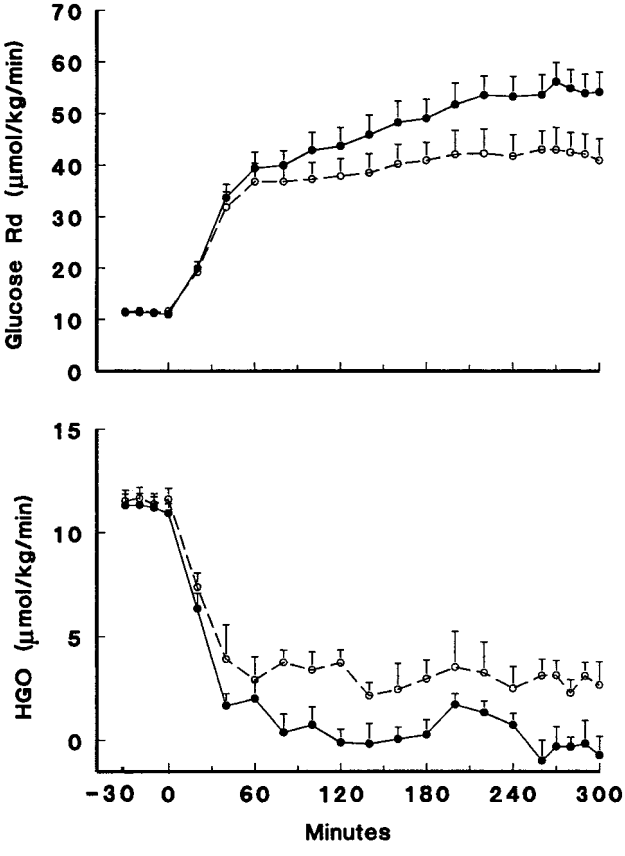

FIG. 1. Rates of whole-body glucose disposal (*top*) and HGO (*bottom*) in 10 normal male subjects in the basal state and during a 5-h 80 mU/m^2·min hyperinsulinemic euglycemic clamp in the absence (Control, ●) and presence (○) of an Intralipid and heparin infusion to raise plasma NEFA levels. Mean ± SEM.

ing the last half hour of the clamp were not significantly different between the two studies (Table 1).

Glucose kinetics

In the basal state, total glucose Rd was similar in the control study (11.2 ± 0.5 μmol/kg·min) and during infusion of Intralipid and heparin (11.6 ± 0.5 μmol/kg·min). Glucose Rd increased nearly 5-fold during the control glucose clamp study (Fig. 1). When plasma NEFAs were elevated by infusion of Intralipid and heparin, the increase in glucose Rd was blunted, and it reached a level during the last 40 min of the glucose clamp that was 24% lower (42.1 ± 4.0) than in the control study (54.8 ± 3.6 μmol/kg·min; $P < 0.001$). The glucose infusion rate that was required to maintain the target plasma glucose level during the last 40 min of the clamp was 28% lower when NEFAs were elevated (39.8 ± 4.2 *vs.* 55.1 ± 4.0 μmol/kg·min; $P < 0.001$). Although elevated NEFA resulted in a decrease in insulin-stimulated glucose Rd in all subjects, the magnitude of this effect varied considerably between subjects, ranging from a 7–50% decrease in glucose Rd by comparison with the saline control study. The percentage reduction in glucose Rd (compared with the control study) correlated with the plasma NEFA concentrations attained during the last 30 min of the Intralipid study glucose clamps ($r = 0.70$; $P < 0.05$) but not significantly with plasma triglyceride levels ($r = 0.58$; NS).

HGO was completely suppressed after 60 min in the control glucose clamp studies but not when plasma NEFAs were elevated (Fig. 1). During the last 40 min of the clamp (260–300 min), HGO was significantly higher during the Intralipid study (2.8 ± 0.5 μmol/kg·min) than in the control study (−0.4 ± 0.5 μmol/kg·min; $P < 0.01$).

Substrate oxidation

After an overnight fast, when plasma NEFAs were elevated by the Intralipid infusion, basal rates of lipid oxidation were higher than on the control study day (0.84 ± 0.08 *vs.* 0.52 ± 0.11 mg/kg·min; $P < 0.01$), whereas carbohydrate oxidation rates were lower (7.6 ± 0.8 *vs.* 9.0 ± 0.7 μmol/kg·min; $P < 0.05$). During the glucose clamps with elevated NEFA, both the suppression of lipid oxidation and the enhancement of glucose oxidation were impaired. During the last 40 min of the glucose clamps, lipid oxidation was significantly higher in the Intralipid study than during the control study (0.51 ± 0.07 *vs.* 0.03 ± 0.02 mg/kg·min; $P < 0.001$) whereas glucose oxidation rates were lower (15.3 ± 0.5 *vs.* 22.4 ± 1.2 μmol/kg·min; $P < 0.001$). Nonoxidative glucose Rd during the last 40 min of the clamps was also significantly lower when NEFAs were elevated (26.8 ± 3.9 *vs.* 32.4 ± 2.8 μmol/kg·min; $P < 0.05$). Thus, of the total defect in glucose Rd during the Intralipid study, 55% was due to a decrease in glucose oxidation, and 45% was due to a decrease in nonoxidative metabolism.

Muscle protein levels

Skeletal muscle levels of the IR-β and IR phosphorylation at the end of the clamps were unaffected by lipid infusion (data not shown). Basal skeletal muscle IRS-1 levels were the same in the control and Intralipid studies (Fig. 2). In the control study, IRS-1 levels decreased by 40% during

the clamp ($P < 0.005$), whereas no decline in IRS-1 levels occurred during the Intralipid study (Fig. 2). Tyrosine phosphorylated IRS-1 in the muscle lysates increased by 29% during the control glucose clamp studies ($P < 0.05$), but increased by only 18% (NS) during the Intralipid clamp study (Fig. 2). Because total IRS-1 levels fell during the control glucose clamp studies, it is apparent that the stoichiometry of IRS-1 tyrosine phosphorylation increased to an even greater extent in the control clamp study. As seen in Fig. 2, tyrosine phosphorylated IRS-1 expressed per unit of IRS-1 increased by 92% ($P < 0.005$), whereas in the Intralipid study the much smaller increase did not reach statistical significance.

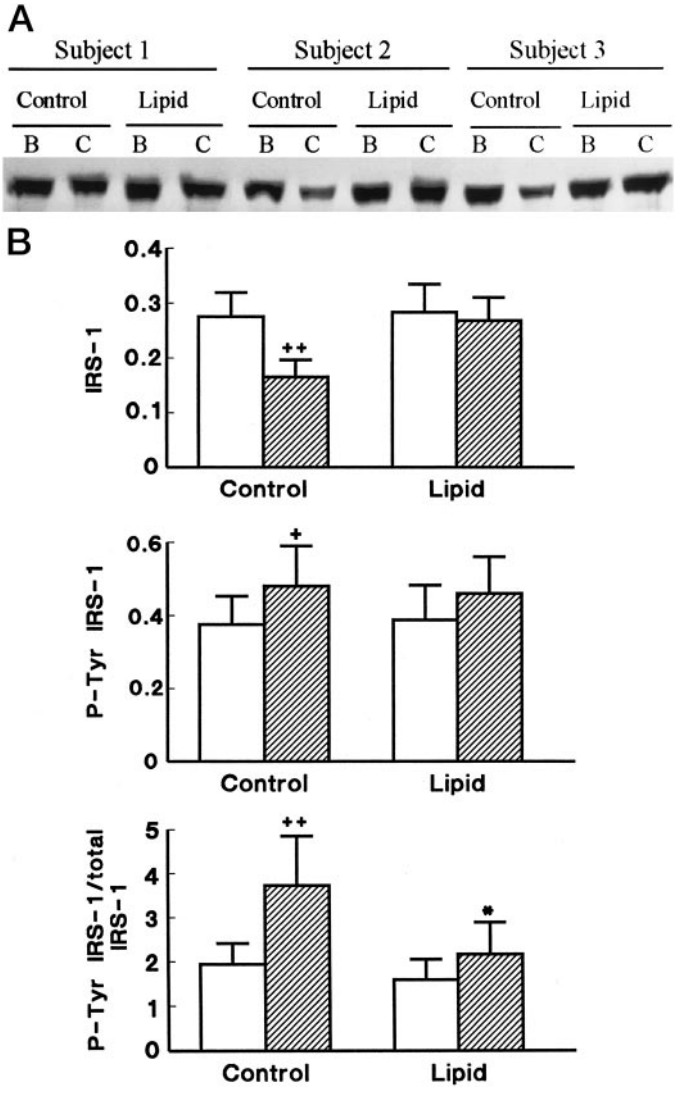

FIG. 2. A, Representative Western blot for IRS-1 protein in muscle samples obtained from three of the subjects in the basal state (*B*) and at the end of the 5-h 80 mU/m^2·min hyperinsulinemic euglycemic clamps (*C*). In subjects 2 and 3, a reduction in the IRS-1 signal in the control glucose clamp sample compared with that in the basal state is clearly seen, whereas in subject 1 the decrease was much less. B, Skeletal muscle IRS-1 protein levels relative to levels of IRS-1 in a standard 3T3-L1 lysate (*top*), muscle tyrosine-phosphorylated IRS-1 levels relative to levels of tyrosine-phosphorylated IRS-1 in a standard 3T3-L1 lysate (*middle*), and tyrosine-phosphorylated IRS-1 normalized to IRS-1 levels (*bottom*) in the 10 normal subjects in the basal state (*white bars*) and at the end of the 5-h 80 mU/m^2·min hyperinsulinemic euglycemic clamps (*shaded bars*) in the absence and presence of Intralipid and heparin. Arbitrary units are used on y-axis. Mean ± SEM. +, $P < 0.05$, and ++, $P < 0.005$ *vs.* basal levels; *, $P < 0.05$compared with the control study.

Skeletal muscle levels of the p85α subunit of PI3K in muscle lysates were the same in the basal state and at the end of the clamp in both studies (data not shown). Total skeletal muscle Akt protein levels were also the same during the two studies and were unaffected by the glucose clamps (control study, basal, 0.69 ± 0.08 U; end of clamp, 0.69 ± 0.09 U; lipid study, basal 0.87 ± 0.18 U; end of clamp, 0.92 ± 0.11 U; NS). As seen in Fig. 3, the hyperinsulinemic glucose clamps resulted in a marked increase in P-ser and P-thr Akt levels, and the effect was the same in the control and Intralipid studies.

PI3K activity

Basal skeletal muscle IRS-1-associated PI3K activity was not affected by elevation of plasma NEFA levels (Fig. 4). At

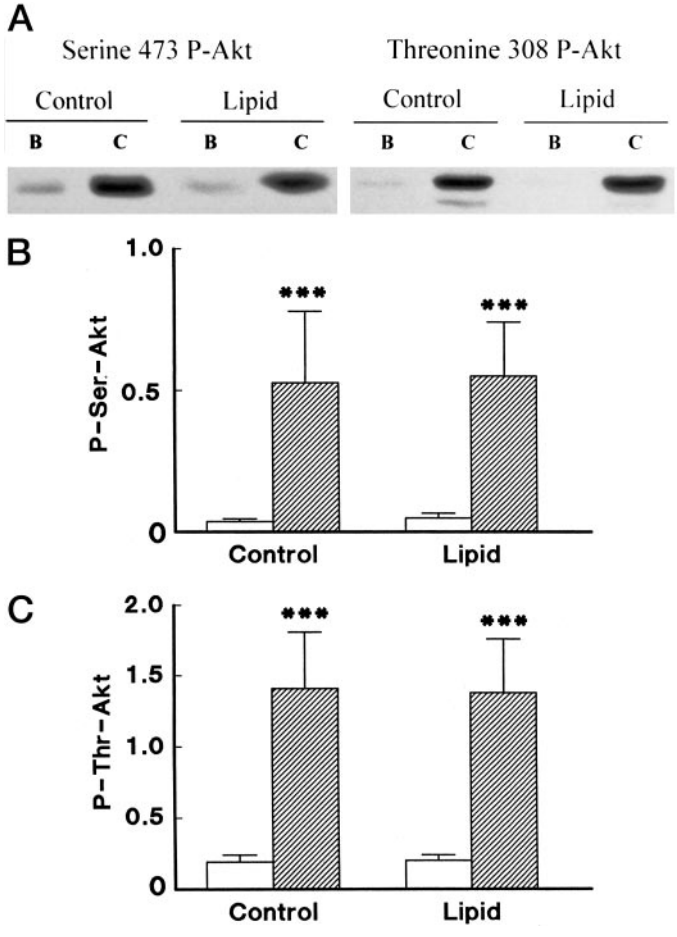

FIG. 3. A, Representative Western blot for serine 473P-Akt and threonine 308P-Akt in muscle taken from one of the subjects in the basal state (*B*) and at the end of the hyperinsulinemic euglycemic clamps (*C*). B, Skeletal muscle P-serine Akt (*top*) and P-threonine Akt (*bottom*) relative to levels in a standard 3T3-L1 lysate in the 10 normal subjects in the basal state (*white bars*) and at the end of the 5-h 80 mU/m^2·min hyperinsulinemic euglycemic clamps (*shaded bars*) in the absence and presence of an Intralipid and heparin infusion. Arbitrary units are used on y-axis. Mean ± SEM. ***, $P < 0.001$ *vs.* basal levels.

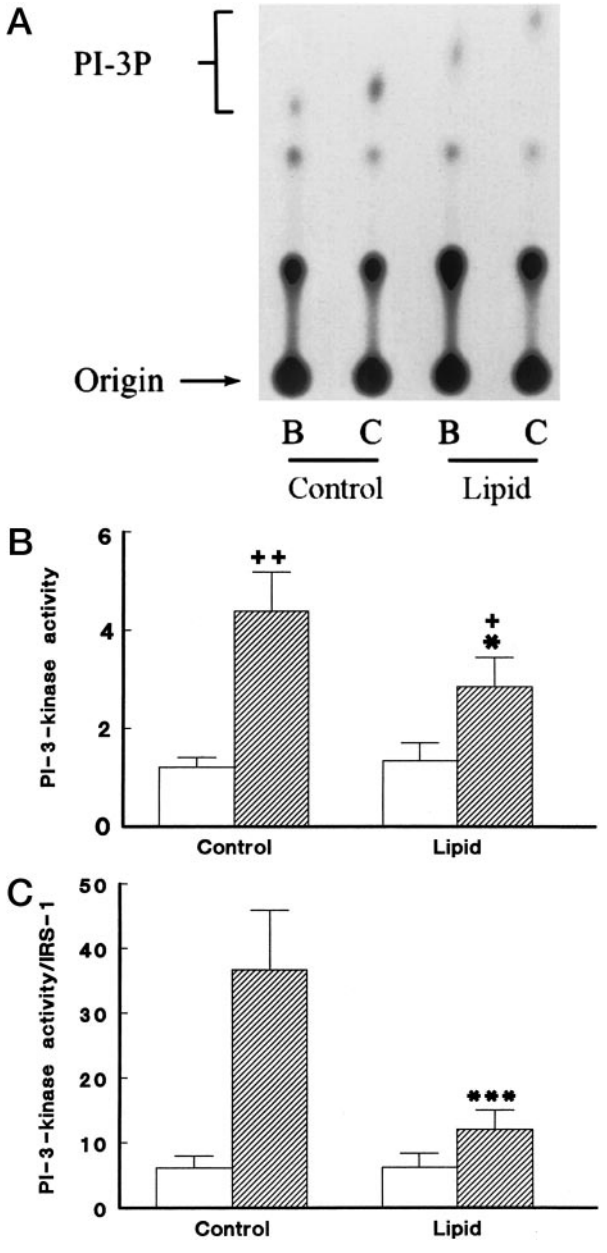

FIG. 4. PI3K data. A, A representative subject's autoradiogram of a TLC plate showing incorporation of ^{32}P into the 3′ position of phosphatidyl inositol. *B*, Basal; *C*, end of 80 mU/m^2·min hyperinsulinemic glucose clamp. B, Skeletal muscle PI3K activity in the 10 normal subjects in the basal state (*white bars*) and at the end of the 5-h 80 mU/m^2·min hyperinsulinemic euglycemic clamps (*shaded bars*) in the absence and presence of an Intralipid and heparin infusion. Data are in arbitrary units normalized to the PI3K activity in one subject's muscle sample at the end of the control glucose clamp study. Mean ± SEM. *, $P < 0.05$ compared with values at the end of the control glucose clamp. +, $P < 0.05$, and ++, $P < 0.002$, compared with corresponding basal values. C, Skeletal muscle PI3K activity in the 10 subjects normalized to IRS-1 levels. Legend as in B. Arbitrary units are used on y-axis. Mean ± SEM. ***, $P < 0.005$ *vs.* control study.

the end of the control glucose clamps, muscle IRS-1-associated PI3K was increased 5.0 ± 1.5-fold (Fig. 4B) ($P < 0.002$). During the glucose clamps with Intralipid, the increase in IRS-1-associated PI3K activity was blunted (3.7 ± 1.6-fold) ($P < 0.05$), and at the end of the clamp the activity was 35% lower (2.85 ± 0.59) than in the control study (4.38 ± 0.80) ($P < 0.05$). Because IRS-1 levels were down-regulated by the insulin infusion in the control but not in the Intralipid glucose clamp studies, the difference in PI3K activity at the end of the glucose clamps was even more marked when normalized to muscle IRS-1 levels (Fig. 4C) ($P < 0.005$). Although, muscle PI3K activity did not correlate with the insulin sensitivity of the subjects as measured by the control glucose clamp, a significant relationship was found between the percentage reduction in PI3K activation and the reduction in insulin-stimulated glucose Rd induced by elevated NEFA ($r = 0.70$; $P < 0.05$) (Fig. 5).

Discussion

The mechanism by which NEFAs induce peripheral insulin resistance remains unclear. Roden *et al.* (7) and Dresner *et al.* (12), using nuclear magnetic resonance spectroscopy to measure muscle glucose-6-phosphate levels and the muscle intracellular free glucose concentration during glucose clamps with and without elevated plasma NEFA, have produced compelling evidence to indicate that the time-dependent reduction of insulin-stimulated glucose disposal seen with elevated NEFA cannot simply be due to a downstream block in glucose metabolism, as originally hypothesized by Randle *et al.* (36), but must involve an additional primary defect in the pathway by which insulin stimulates muscle glucose transport. Altered Glut 4 expression does not appear to play a role (37). Several *in vitro* studies have suggested that fatty acids may affect the insulin-signaling pathway between the IR and Akt, although the findings differ between studies (23, 38). Storz *et al.* (23) found that in cultured myoblasts, palmitate decreased insulin-stimulated tyrosine phosphorylation of the IR-β. By contrast, Gumbiner *et al.* (13) found that in normal subjects insulin binding and basal and insulin-stimulated insulin receptor kinase activity were unaffected by elevated NEFA, and they suggested that the NEFA-induced defect in insulin signaling was downstream of the insulin receptor. Dresner *et al.* (12) found that NEFA-induced

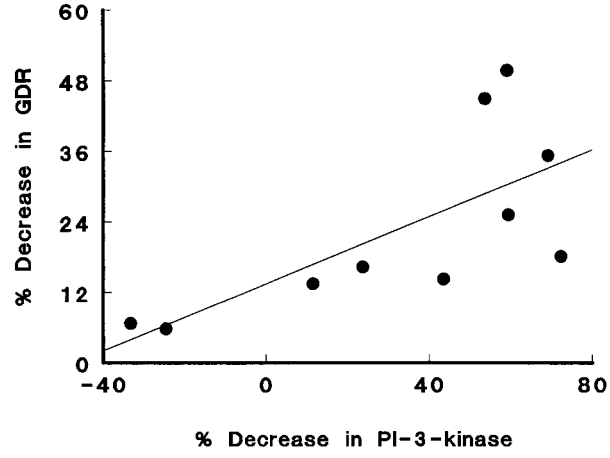

FIG. 5. Relationship between the percentage reduction in PI3K activation by insulin during the clamps with elevated NEFA compared with the control glucose clamp study and the reduction in insulin-stimulated glucose Rd induced by elevated NEFA ($r = 0.70$; $P < 0.05$) in the 10 male subjects.

insulin resistance in normal subjects was associated with a marked decrease in IRS-1-associated PI3K activity. However, levels of insulin-signaling proteins and effects on IR-β and IRS-1 tyrosine phosphorylation were not examined. In this study, we sought to examine the effects of a physiological elevation of plasma NEFA on proximal insulin-signaling steps thought to be important for the stimulatory effect of insulin on glucose transport.

Elevated plasma NEFA resulted in a 24% decrease in total insulin-stimulated glucose Rd, due to a reduction in both oxidative and nonoxidative glucose Rd. Suppression of HGO during the glucose clamps with elevated NEFA was also impaired, although we used a rather high insulin infusion rate that resulted in plasma insulin levels around 720 pmol/liter (120 mU/liter) (Fig. 1). Because the Intralipid and heparin were started 2.5 h before the glucose clamps, these defects were already apparent during the second hour of the clamps (Fig. 1). The degree of insulin resistance induced by elevated plasma NEFA is generally consistent with that found by others (3, 8, 10–14), and a good correlation was found between the percentage reduction in glucose Rd and the plasma NEFA concentrations during the last 30 min of the glucose clamps with Intralipid ($r = 0.70$; $P < 0.05$).

Elevated NEFA had no effect on basal or insulin-stimulated muscle IR-β levels or their level of tyrosine phosphorylation as determined by Western blotting. These findings concur with those of Gumbiner *et al.* (13), who found no effect of elevated NEFA on muscle insulin receptor kinase activity, and are consistent with the view that NEFAs impair insulin signaling downstream of the insulin receptor. A key finding in our study is that when NEFAs were elevated during the glucose clamps, the insulin-induced increase in IRS-1-associated PI3K activity was blunted (Fig. 4). Moreover, the magnitude of this defect correlated with the reduction in insulin-stimulated glucose Rd induced by elevated NEFA ($r = 0.70$; $P < 0.05$) (Fig. 5).

The 35% reduction in IRS-1-associated PI3K activity at the end of the Intralipid clamps, compared with the control clamps, is less than the defect reported by Dresner *et al.* (12). The higher lipid infusion rate and NEFA levels in that study and the greater degree of insulin resistance induced could explain this difference. Another factor, however, could be the timing of the muscle biopsy that was performed 30 min after the start of the insulin infusion in their study (12). The extent of activation of PI3K may wane with prolonged insulin exposure (39, 40). Fasshauer *et al.* (41) found that in brown adipocytes from IRS-2 knockout mice, a 30% reduction in total phosphotyrosine-associated PI3K activity was associated with an impairment of Glut 4 translocation and a 50% decrease in insulin-induced glucose uptake. In view of the evidence that NEFA-induced insulin resistance involves a defect of muscle glucose transport (7, 12), it seems likely that the 35% reduction in IRS-1-associated PI3K activity at the end of the Intralipid clamps led to a defect of muscle Glut 4 translocation that in turn resulted in a decrease in total glucose Rd.

PI3K is activated by the binding of its regulatory p85 subunit to tyrosine-phosphorylated IRS-1. Thus, an impairment of IRS-1 phosphorylation on tyrosines would explain the decreased activation of PI3K by insulin. Interpretation of our tyrosine-phosphorylated IRS-1 data must take into account the higher muscle IRS-1 protein levels at the end of the clamps with elevated NEFA compared with the control study (Fig. 2). Thus, although the tyrosine-phosphorylated IRS-1 signal in the whole muscle lysate was not significantly different at the end of the control and Intralipid clamps, the stoichiometry of IRS-1 tyrosine phosphorylation was clearly altered by the increased NEFA levels (Fig. 2). The data are compatible with either a smaller proportion of IRS-1 molecules that are tyrosine phosphorylated or with the presence of less heavily phosphorylated IRS-1 species in the lipid study. In rats, the defect in IRS-1 phosphorylation induced by elevated NEFA was found to be associated with increased membrane PKC θ levels (24), raising the possibility that increased serine-threonine phosphorylation of IRS-1 by this PKC isoform may make IRS-1 a poorer substrate for the insulin receptor kinase (42, 43). This may result in a subpopulation of IRS-1 molecules that are not tyrosine phosphorylated or may impair the phosphorylation of specific sites on IRS-1. Either way, a PKC mechanism would fit with our data. Serine phosphorylation of IRS-1 might be expected to retard the mobility of IRS-1 on the SDS-gels. However, we did not observe any effect of elevated NEFA on IRS-1 mobility.

An alteration in the specific IRS-1 tyrosines phosphorylated in the clamps with Intralipid could readily explain the impairment of PI3K activation by insulin although the total phosphotyrosine IRS-1 signal was not significantly decreased. For example, if the particular p85 binding sites on IRS-1 were phosphorylated to a lesser extent, because of increased PKC activity or some other mechanism, then this would explain why less PI3K was immunoprecipitated by the IRS-1 antibody.

Muscle IRS-1 protein levels were 40% lower at the end of the control glucose clamps than in the basal state ($P < 0.005$). Down-regulation of IRS-1 protein levels by prolonged exposure (4 h or more) to high insulin levels has been reported in Chinese hamster ovary cells overexpressing human insulin receptors and IRS-1 (44). Interestingly, although basal IRS-1 levels were not affected by elevated NEFA, the down-regulation of IRS-1 during the glucose clamps was completely prevented (Fig. 2). The insulin-induced down-regulation of IRS-1 protein levels is thought to be at least partly mediated by the proteasome degradation pathway and to require PI3K activation (44). It is thus possible that the defect of IRS-1 down-regulation seen during the glucose clamps with elevated NEFA could be secondary to the impairment of IRS-1-associated PI3K activation when plasma NEFAs were elevated (Fig. 4).

Most (20, 21, 45, 46) but not all (22, 47) studies support a role for Akt in the effects of insulin on Glut 4 translocation and glucose transport. Akt is a serine/threonine kinase that is downstream of PI3K. It is activated by phosphorylation on thr 308 and ser 473 in Akt 1 (thr 309 and ser 474 in Akt 2) by phospholipid-dependent kinase-1 (48). PI-3-P, the major lipid product of the PI3K reaction, promotes this phosphorylation by phospholipid-dependent kinase-1 by binding to the amino terminus of Akt (48, 49). In *in vitro* cell systems, inhibitors of PI3K block the activation of Akt (19, 48). As expected, insulin induced a marked increase in the phos-

phorylation of Akt at both ser 473 and thr 308. However, despite the 35% decrease in IRS-1-associated PI3K activity at the end of the Intralipid glucose clamps compared with the control glucose clamp studies, no impairment of Akt phosphorylation at either thr 308 or ser 473 was found (Fig. 3). There are several potential explanations for the seemingly divergent effects of elevated NEFA on insulin stimulation of IRS-1-associated PI3K activity and the phosphorylation of Akt. Firstly, only partial activation of PI3K may be necessary for full stimulation of Akt. Secondly, changes in total IRS-1-associated PI3K activity and Akt phosphorylation may not reflect changes within specific membrane compartments (41, 50). Thirdly, a PI3K-independent mechanism for activation of Akt (51, 52) may be able to offset the 35% decrease in IRS-1-associated PI3K activity. A similar dissociation between effects on PI3K activity and on Akt has been observed in other insulin-resistant states. Thus, glucosamine-induced insulin resistance in rats was accompanied by a smaller increase in muscle IRS-1-associated PI3K activity in response to an acute insulin stimulus but no change in Akt activity (40).

It has been proposed that Akt 2 rather than Akt 1 is involved in insulin-induced glucose uptake, because Akt 2 but not Akt 1 was found to colocalize with Glut 4-containing vesicles and to redistribute to the plasma membrane of rat fat cells in response to insulin (41). The antibody used in our study recognizes both Akt 1 and Akt 2. Thus, it is conceivable that a small difference, specifically in Akt 2 phosphorylation, went undetected. However, our data concur with those of Fasshauer *et al.* (41). These investigators found that in brown adipocytes from IRS-2 knockout mice, phosphorylation and activation of both Akt 1 and Akt 2 was normal, despite a 30% decrease in phosphotyrosine-associated PI3K activity. Interestingly, despite normal total Akt phosphorylation and activation, translocation of Akt to the plasma membrane was impaired in the adipocytes from the IRS-2 knockout mice (41).

The findings in our study must take into account the fatty acid composition of the infused Intralipid, which differs significantly from that of plasma (13% linoleate, 27% palmitate, 35% oleate, 12% stearate, 12% other) (53). It has been suggested that palmitate has a greater propensity for inducing insulin resistance than other fatty acids (23). However, in another study, linoleate, oleate, and palmitate had similar inhibitory effects on glycogen synthesis and 2-deoxyglucose uptake in cultured mouse myotubes, although their specific effects on proximal insulin-signaling steps differed (38). *In vivo* studies have also indicated that fatty acids other than palmitate, particularly linoleate, can induce muscle insulin resistance (54).

In conclusion, insulin resistance induced by a physiological elevation of plasma NEFA levels was associated with an abnormality of muscle IRS-1 tyrosine phosphorylation and a defect in insulin activation of IRS-1-associated PI3K activity. Muscle IRS-1 down-regulation by insulin was also impaired by elevated NEFA levels. The defect in PI3K activation by insulin correlated with the reduction in whole-body glucose disposal induced by elevated NEFA. Because activation of PI3K is necessary for insulin-induced Glut 4 translocation, our data support the notion that the NEFA-induced impairment of insulin-stimulated muscle glucose uptake is, at least in part, a consequence of defects in the insulin-signaling pathway leading to impaired PI3K activation. However, insulin-induced phosphorylation of Akt was unaffected by elevated NEFA. Assuming that insulin-induced translocation of Akt to Glut 4 vesicles and the plasma membrane parallels the phosphorylation and activation of total cellular Akt, our data would suggest that this downstream effector of PI3K may not participate in the NEFA-induced defect of muscle glucose uptake and that alternative PI3K-dependent pathways may be involved (55, 56).

Acknowledgments

Received October 10, 2000. Accepted July 30, 2001.

Address all correspondence and requests for reprints to: Yolanta Kruszynska, M.D., Department of Endocrinology and Metabolism (9111G), Veterans Administration Medical Center, 3350 La Jolla Village Drive, La Jolla, California 92093.

This study was supported by the Whittier Institute, NIH Grant DK 33649, General Clinical Research Center Grant RR00827, and the Medical Service, Department of Veterans Affairs, Veterans Administration Medical Center, San Diego, California.

References

1. **Randle PJ** 1998 Regulatory interactions between lipids and carbohydrates: the glucose fatty acid cycle after 35 years. Diabetes Metab Rev 14:263–283
2. **McGarry JD** 1992 What if Minkowski had been ageusic? An alternative angle on diabetes. Science 258:766–770
3. **Kruszynska YT** 1995 The role of fatty acid metabolism in the hypertriglyceridaemia and insulin resistance of Type 2 (non-insulin dependent) diabetes. In: Marshall SM, Home PD, Rizza RA, eds. The diabetes annual. 9:107–139
4. **Perseghin G, Ghosh S, Gerow K, Shulman GI** 1997 Metabolic defects in lean nondiabetic offspring of NIDDM parents. A cross sectional study. Diabetes 46:1001–1009
5. **Baldeweg SE, Golay A, Natali A, Balkau B, Del Prato S, Coppack SW** 2000 Insulin resistance, lipid and fatty acid concentrations in 867 healthy Europeans. Eur J Clin Invest 30:45–52
6. **Paolisso G, Tataranni PA, Foley JE, Bogardus C, Howard BV, Ravussin E** 1995 A high concentration of fasting plasma non-esterified fatty acids is a risk factor for the development of NIDDM. Diabetologia 38:1213–1217
7. **Roden M, Price TB, Perseghin G, Petersen KF, Rothman DL, Cline GW, Shulman GI** 1996 Mechanism of free fatty-acid induced insulin resistance in humans. J Clin Invest 97:2859–2865
8. **Bonadonna RC, Zych K, Boni C, Ferrannini E, DeFronzo RA** 1989 Time dependence of the interaction between lipid and glucose in humans. Am J Physiol 257:E49–E56
9. **Groop LC, Bonadonna RC, Shank M, Petrides AS, DeFronzo RA** 1991 Role of free fatty acids and insulin in determining free fatty acid and lipid oxidation in man. J Clin Invest 87:83–89
10. **Lee KU, Lee HK, Koh CS, Min HK** 1988 Artificial induction of intravascular lipolysis by lipid-heparin infusion leads to insulin resistance in man. Diabetologia 31:285–290
11. **Boden G, Chen X, Ruiz J, White JV, Rossetti L** 1994 Mechanisms of fatty acid-induced inhibition of glucose uptake. J Clin Invest 93:2438–2446
12. **Dresner A, Laurent D, Marcucci M, Griffin ME, Dufour S, Cline SW, Slezak LA, Andersen DK, Hundal RS, Rothman DL, Petersen KF, Shulman GI** 1999 Effects of free fatty acids on glucose transport and IRS-1-associated phosphatidylinositol 3-kinase activity. J Clin Invest 103:253–259
13. **Gumbiner B, Mucha JF, Lindstrom JE, Rekhi I, Livingston JN** 1996 Differential effects of acute hypertriglyceridemia on insulin action and insulin receptor autophosphorylation. Am J Physiol 270:E424–E429
14. **Thiebaud D, DeFronzo RA, Jacot E, Golay A, Acheson K, Maeder E, Jequier E, Felber J-P** 1982 Effect of long chain triglyceride infusion on glucose metabolism in man. Metabolism 31:1128–1136
15. **Kim JK, Youn JH** 1997 Prolonged suppression of glucose metabolism causes insulin resistance in rat skeletal muscle. Am J Physiol 272:E288–E296
16. **Randle PJ, Newsholme EA, Garland PB** 1964 Regulation of glucose uptake by muscle. Effects of fatty acids, ketone bodies, pyruvate, and of alloxan-diabetes and starvation, on the uptake and metabolic fate of glucose in rat heart and diaphragm muscles. Biochem J 93:652–665
17. **Roden M, Krssak M, Stingl H, Gruber S, Hofer A, Furnsinn C, Moser E, Waldhausl W** 1999 Rapid impairment of skeletal muscle glucose transport/phosphorylation by free fatty acids in humans. Diabetes 48:358–364

18. **Virkamaki A, Ueki K, Kahn RC** 1999 Protein-protein interaction in insulin signaling and the molecular mechanisms of insulin resistance. J Clin Invest 103:931–943
19. **Shepherd PR, Withers DJ, Siddle K** 1998 Phosphoinositide 3-kinase: the key switch mechanism in insulin signalling. Biochem J 333:471–490
20. **Foran PGP, Fletcher LM, Oatey PB, Mohammed N, Dolly JO, Tavare JM** 1999 Protein kinase B stimulates the translocation of Glut 4 but not Glut 1 or transferrin receptors in 3T3-L1 adipocytes by a pathway involving SNAP-23, synaptobrevin-2, and/or cellubrevin. J Biol Chem 274:28087–28095
21. **Hill MM, Clark SF, Tucker DF, Birnbaum MJ, James DE, Macaulay SL** 1999 A role for protein kinase Bβ/Akt2 in insulin-stimulated Glut 4 translocation in adipocytes. Mol Cell Biol 19:7771–7781
22. **Kitamura T, Ogawa W, Sakaue H, Hino Y, Kuroda S, Takata M, Matsumoto M, Maeda T, Konishi H, Kikkawa U, Kasuga M** 1998 Requirement for activation of the serine-threonine kinase Akt (protein kinase B) in insulin stimulation of protein synthesis but not of glucose transport. Mol Cell Biol 18: 3708–3717
23. **Storz P, Doppler H, Wernig A, Pfizenmaier K, Muller G** 1999 Cross-talk mechanisms in the development of insulin resistance of skeletal muscle cells palmitate rather than tumour necrosis factor inhibits insulin-dependent protein kinase B (PKB)/Akt stimulation and glucose uptake. Eur J Biochem 266: 17–25
24. **Griffin ME, Marcucci M, Cline GW, Bell K, Barucci N, Lee D, Goodyear LJ, Kraegen EW, White MF, Shulman GI** 1999 Free fatty acid-induced insulin resistance is associated with activation of protein kinase C theta and alterations in the insulin signaling cascade. Diabetes 48:1270–1274
25. **DeFronzo RA, Tobin JD, Andres R** 1979 Glucose clamp technique: a method for quantifying insulin secretion and resistance. Am J Physiol 237:E214–E223
26. **Bergstrom J** 1962 Muscle electrolytes in man determined by neutron activation analysis on needle biopsy specimen: a study on normal subjects, kidney patients, and patients with chronic diarrhea. Scand J Clin Lab Invest 14(Suppl 68):1–110
27. **Kruszynska YT, Mulford MI, Yu JG, Armstrong DA, Olefsky JM** 1997 Effects of nonesterified fatty acids on glucose metabolism after glucose ingestion. Diabetes 46:1586–1593
28. **Ferrannini E** 1988 The theoretical bases of indirect calorimetry: a review. Metabolism 37:287–301
29. **Ruderman NB, Kapeller R, White MF, Cantley LC** 1990 Activation of phosphatidylinositol 3-kinase by insulin. Proc Natl Acad Sci USA 87:1411–1415
30. **Serunian LA, Auger KR, Cantley LC** 1991 Identification and quantification of polyphosphoinositides produced in response to platelet-derived growth factor stimulation. Methods Enzymol 198:78–87
31. **Somogyi MJ** 1945 Determination of blood sugar. J Biol Chem 160:69–73
32. **Desbuquois B, Aurbach GD** 1971 Use of polyethylene glycol to separate free and antibody bound peptide hormones in radioimmunoassays. J Clin Endocrinol Metab 33:732–738
33. **Thorburn AW, Gumbiner B, Flynn T, Henry RR** 1991 Substrate oxidation errors during combined indirect calorimetry-hyperinsulinemic glucose clamp studies. Metabolism 40:391–398
34. **Steele R** 1959 Influences of glucose loading and of injected insulin on hepatic glucose output. Ann NY Acad Sci 82:420–430
35. **Wolfe RR** 1984 Tracers in metabolic research: radioisotope/mass spectrometry methods. New York: Liss; 81–101
36. **Randle PJ, Garland PB, Hales CN, Newsholme EA** 1963 The glucose-fatty acid cycle: its role in insulin sensitivity and the metabolic disturbances of diabetes mellitus. Lancet i:785–789
37. **Magnan C, Gilbert M, Kahn BB** 1996 Chronic free fatty acid infusion in rats results in insulin resistance but no alteration in insulin-responsive glucose transporter levels in skeletal muscle. Lipids 31:1141–1149
38. **Schmitz-Peiffer C, Craig DL, Biden TJ** 1999 Ceramide generation is sufficient to account for the inhibition of the insulin-stimulated PKB pathway in C2C12 skeletal muscle cells pretreated with palmitate. J Biol Chem 274:24202–24210
39. **Song XM, Ryder JW, Kawano Y, Chibalin AV, Krook A, Zierath JR** 1999 Muscle fiber type specificity in insulin signal transduction. Am J Physiol 277:R1690–R1696
40. **Kim Y-B, Zhu J-S, Zierath JR, Shen H-Q, Baron AD, Kahn BB** 1999 Glucosamine infusion in rats rapidly impairs insulin stimulation of phosphoinositide 3-kinase but does not alter activation of Akt/protein kinase B in skeletal muscle. Diabetes 48:310–320
41. **Fasshauer M, Klein J, Ueki K, Kriauciunas KM, Benito M, White MF, Kahn RC** 2000 Essential role of IRS-2 in insulin stimulation of Glut 4 translocation and glucose uptake in brown adipocytes. J Biol Chem 275:25494–25501
42. **De Fea K, Roth RA** 1997 Protein kinase C modulation of insulin receptor substrate-1 tyrosine phosphorylation requires serine 612. Biochemistry 36: 12939–12947
43. **Ravichandran LV, Esposito DL, Chen J, Quon MJ** 2001 PKC-zeta phosphorylates IRS-1 and impairs its ability to activate P-3-kinase in response to insulin. J Biol Chem 276:3543–3549
44. **Sun XJ, Goldberg JL, Qiao L, Mitchell JJ** 1999 Insulin-induced insulin receptor substrate-1 degradation is mediated by the proteasome degradation pathway. Diabetes 48:1359–1364
45. **Celera MR, Martinez C, Liu H, El Jack AK, Birnbaum MJ, Pilch PF** 1998 Insulin increases the association of Akt-2 with Glut4-containing vesicles. J Biol Chem 273:7201–7204
46. **Tanti J-F, Grillo S, Gremeaux T, Coffer PJ, Van Obberghen E, Le Marchand-Brustel Y** 1997 Potential role of protein kinase B in glucose transporter 4 translocation in adipocytes. Endocrinology 138:2005–2010
47. **Imamura T, Vollenweider P, Egawa K, Clodi M, Ishibashi K, Nakashima N, Ugi S, Adams JW, Brown JH, Olefsky JM** 1999 G alpha-q/11 protein plays a key role in insulin-induced glucose transport in 3T3–L1 adipocytes. Mol Cell Biol 19:6765–6774
48. **Meier R, Hemings BA** 1999 Regulation of protein kinase B. J Recept Signal Transduct Res 19:121–129
49. **Stokoe D, Stephens LR, Copeland T, Gaffney PRJ, Reese CB, Painter GF, Holmes AB, McCormick F, Hawkins PT** 1997 Dual role of phosphatidylinositol-3,4,5-triphosphate in the activation of protein kinase B. Science 277:567–570
50. **Inoue G, Cheatham B, Emkey R, Kahn CR** 1998 Dynamics of insulin signaling in 3T3-L1 adipocytes. Differential compartmentalization and trafficking of insulin receptor substrate (IRS)-1 and IRS-2. J Biol Chem 273:11548–11555
51. **Moule SK, Welsh GI, Edgell NJ, Foulstone EJ, Proud CG, Denton RM** 1997 Regulation of protein kinase B and glycogen synthase kinase-3 by insulin and beta-adrenergic agonists in rat epididymal fat cells. Activation of protein kinase B by wortmannin-sensitive and -insensitive mechanisms. J Biol Chem 272:7713–7719
52. **Yano S, Tokumistu H, Soderling TR** 1998 Calcium promotes cell survival through CaM-K kinase activation of the protein kinase B pathway. Nature 396:584–587
53. **Hagenfeldt L, Wahren J, Pernow B, Raf L** 1972 Uptake of individual free fatty acids by skeletal muscle and liver in man. J Clin Invest 51:2324–2330
54. **Storlien LH, Kraegen EW, Chisholm DJ, Ford GL, Bruce DG, Pascoe WS** 1987 Fish oil prevents insulin resistance induced by high-fat feeding in rats. Science 237:885–888
55. **Elmendorf JS, Pessin JE** 1999 Insulin signaling regulating the trafficking and plasma membrane fusion of Glut 4 - containing intracellular vesicles. Exp Cell Res 253:55–62
56. **Kotani K, Ogawa W, Matsumoto M, Kitamura T, Sakaue H, Hino Y, Miyake K, Sano W, Akimoto K, Ohno S, Kasuga M** 1998 Requirement of atypical protein kinase Cλ for insulin stimulation of glucose uptake but not for Akt activation in 3T3-L1 adipocytes. Mol Cell Biol 18:6971–6982